Cell Biochem Biophys (2012) 63:35–45
DOI 10.1007/s12013-012-9339-0

ORIGINAL PAPER

What is the Functional Role of N-terminal Transmembrane Helices in the Metabolism Mediated by Liver Microsomal Cytochrome P450 and its Reductase?

Daniel Andrew Gideon · Rashmi Kumari · Andrew M. Lynn · Kelath Murali Manoj

Published online: 1 February 2012

Abstract We sought to clarify on the hitherto unresolved role of N-terminal transmembrane segments (TMS) of cytochrome P450 (CYP) and its' reductase (CPR) in protein interaction/catalysis. TMS analyses show little evolutionary conservation in CYPs. The conserved CPR's TMS poses limited scope for predictable/consistent hetero-recognition with the wide bevy of CYPs' TMS, as evident from preliminary analyses and TM*hit* server predictions for inter-helical binding. Further, experimentations with four different CPR preparations (preps) and two liver microsomal CYPs (2C9 and 2E1) shows that the hydroxylated product formation rate is not quantitatively correlated to the extent of integrity of the CPR N-terms. Incorporation of cytochrome b_5 in some reactions afforded similar rates while employing either fully intact or partially intact CPR. A survey of literature shows that liver microsomal CYPs function quite well even without the TMS or with significantly altered TMS. These observations negate the hypothesis that N-term TMS of CPR or CYP is obligatory for CYP–CPR interaction and catalysis. Also, in CYP2E1-mediated hydroxylation of *para*-nitrophenol, the extent of intactness or truncation did not significantly affect the CPR preps' catalytic role at very low or high substrate concentrations. To interpret these results, we draw support from recently published research on reduced nicotinamide adenide dinucleotide phosphate oxidase (Takac et al., J Biol Chem, 286:13304–13313, 2011) and from our pertinent earlier works. We infer that CPR' free TMS segment could alter the diffusible reactive oxygen species' dynamics in the microenvironment, thereby altering the reaction outcome. Based on the evidence, we conclude that TMS merely facilitates "interaction/catalysis" by anchoring the CYP and CPR in the lipid interface.

Keywords Helical interactions · CYP · Hetero-recognition · Membrane anchoring · Liver microsomes

Abbreviations

CYP	Cytochrome P450
CPR	NADPH-cytochrome P450 reductase
NADPH	Reduced nicotinamide adenide dinucleotide phosphate
TMS	Transmembrane segment
TMH	Transmembrane helix
CO	Carbon monoxide
OD	Optical density
DLPC	Dilauryl phosphatidylcholine
HPLC	High performance liquid chromatography
pNC	*Para*-nitrocatechol
pNP	*Para*-nitrophenol
SDS-PAGE	Sodium dodecyl sulfate polyacrylamide gel electrophoresis
Nox	NADPH oxidase
DROS	Diffusible reduced oxygen species

Electronic supplementary material The online version of this article (doi:10.1007/s12013-012-9339-0) contains supplementary material, which is available to authorized users.

D. A. Gideon · K. M. Manoj (✉)
Heme & Flavo Proteins Laboratory, Center for Biomedical Research, VIT University, #204, Vellore 632014, Tamil Nadu, India
e-mail: muralimanoj@vit.ac.in; satyamjayatu@yahoo.com

R. Kumari · A. M. Lynn
School of Computational and Integrative Sciences, Jawaharlal Nehru University, New Delhi, India

Introduction

In the liver microsomal system, two proteins working in tandem carry out the major step (Phase I) in redox metabolism of a wide variety of drugs and xenobiotics. The two enzymes involved are (a) cytochrome P450s (CYPs), a diverse family of heme-thiolate proteins (of ~50 kDa) and (b) cytochrome P450 reductase (CPR), a highly conserved diflavoenzyme (of ~78 kDa) [1, 2]. These two membrane proteins are distributed at CYP:CPR ratios of >20:1 in the phospholipid microenvironments of endoplasmic reticulae and microsomes [3].

The nature of interactions of these two proteins in situ (or in vitro) has been a matter of intense exploration. Coon's group had reported that N-term portions of trypsinized CPR led to a decrease in the substrate hydroxylation, inhibition of reduced nicotinamide adenide dinucleotide phosphate (NADPH) oxidase (Nox) activity and gave perturbed Type-I binding spectra [4, 5 and several references mentioned therein]. They proposed that the inhibitory action exerted by the peptide was by an alleged preference of the CPR's transmembrane segments (TMS) peptide for $CYPLM_2$ (currently known as rabbit CYP2B series). Gum and Strobel had subsequently found that large excesses of the amphiphilic TMS peptide derived by steapsin treatment of CPR did not inhibit the reaction in a reconstituted system [6]. To explain their observations, they postulated that CYP and CPR's TMS serve as a hydrophobic anchor and render the CPR catalytically active or mediate protein–protein interactions. Coon's group also predicted the CPR's N-term to contain a β-sheet structure, which was believed to be involved in P450 and phospholipid binding [7]. There were speculations that the N-terminal sequences of P450s differ in their amino acid composition due to evolutionary pressure as reflected by the statement "the N-terminal section becomes more viable during the elaboration of the phylogenetic tree in response to the evolutionary pressures to metabolize different types of substrate molecules" [8]. Such statements convey the impression that the P450 N-terminal region forms a part of the active site, and thus, amino acid changes in the N-term could influence drug metabolism reactions owing to altered substrate specificities of CYP450s. Müller-Enoch and Gruler [9] said that "the action of catalytic center where the chemical reaction takes place is not influenced by the membrane binding peptide, but the complexation process is influenced by the membrane binding domains." Throughout the past four decades, majority of the workers in the area retained an impression that the N-termini of these two enzymes were crucial to the protein–protein complexation in the reaction mixture [3–13] and interpreted several experimental results to this effect.

The important hypotheses for the role of N-terminal TMS in CYP + CPR interactions/catalysis are depicted in Fig. 1, and are summarized below:

1. The N-termini aid in hetero-recognition/binding, which facilitates CPR-CYP protein–protein electron transfer, which is deemed essential for catalysis.
2. The N-termini (particularly, for CPR) form structural components of the active site in situ, which is obligatory for catalysis.
3. The N-termini play only passive anchors' roles, bringing CYP and CPR in proximity in the phospholipid interface, which facilitates catalysis.

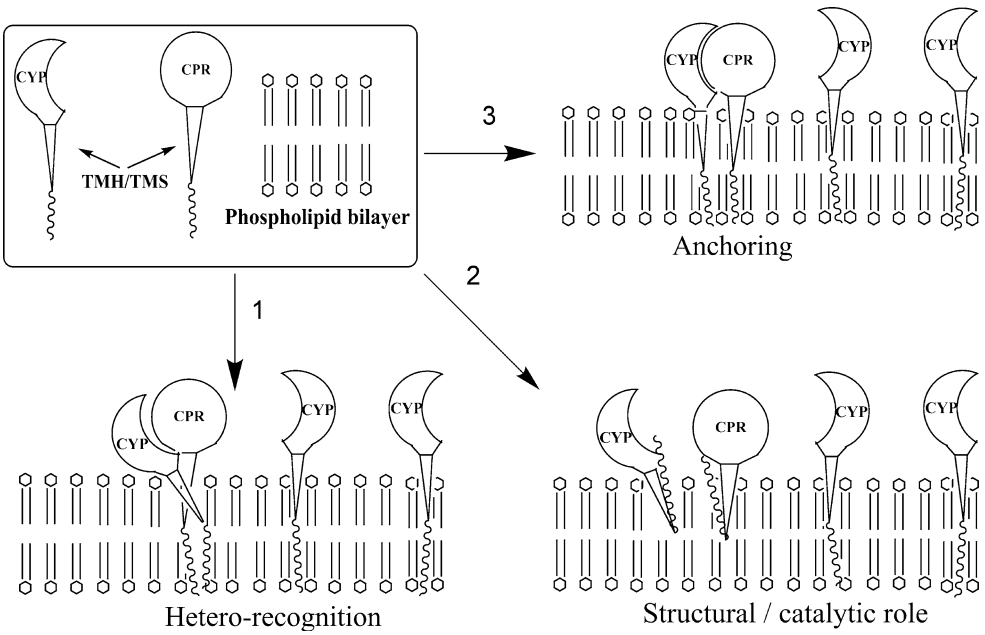

Fig. 1 Probable hypothesis regarding the roles of N-term TMS in CYP + CPR reactions. The *top-left panel* (within the *box*) shows the fundamental components of the reaction system. The three hypotheses under investigation are appropriately labeled therein

Table 1 Determination of TMS of various mammalian CYPs and CPRs using programs (servers) available on internet [14–26]

Algorithm	h1A2	m1A2	r1A2	h2B6	h2C9	h2C19	h2D6	h2E1	m2E1	r2E1	h3A4	hCPR	mCPR	rCPR	References
waveTM	2–28	2–27	2–28	3–20	3–17	3–20	2–20	2–20	2–23	2–23	2–26	25–41	22–38	22–38	[14]
TMPred	9 out–28 in	9 out–29 in	9 out–30 in	3 out–20 in	2 out–20 in	2 out–20 in	5 out 23 in	3 in–21 out	4 out–23 in	2 in–22 out	7 in–27 out	28 out–47 in	22 out–44 in	22 out–43 in	[15]
TopPred	11 out–31 in	9 out–29 in	9 out–29 in	1 out–71 in	1 out–21 in	1 out–21 in	3 out–23 in	1 in–21 out	3 out–23 in	3 in–23 out	7 out–27 in	27 out–47 in	25 out–45 in	24 out–44 in	[16]
DAS	15–30	13–28	11–30	5–23	6–21	7–21	7–24	Short	6–24	8–24	12–28	30–46	25–44	25–45	[17]
SOSUI	7–29	5–27	5–27	l–21	2–23	3–25	3–24	1–21	3–25	3–25	3–24	23–45	20–42	23–44	[18]
TMHMM 2.0	10 out–28 in	5 out–27 in	5 out–27 in	5 out–20 in	4 out–21 in	4 out–21 in	5 out–22 in	2 in–20 out	4 out–23 in	4 out–23 in	7 in–26 out	25 out–47 in	22 out–44 in	22 out–44 in	[19]
pred-tmr	7–28	7–27	8–28	X	X	X	6–23	X	6–23	6–23	12–33	23–41	28–44	28–44	[20]
SMART	10–28	5–27	5–27	5–20	4–21	4–21	5–22	Short	4–23	4–23	7–26	25–47	22–44	22–44	[21]
SPLIT4	1 out–28 in	12 out–30 in	9 out–29 in	1 out–21 in	2 out–20 in	3 out–20 in	l out–22 in	1 in–21 out	1 out–24 in	l out–24 in	5 out–28 in	21 out–44 in	20 out–41 in	20 out–43 in	[22]
tmmod	9 out–28 in	7 out–27 in	9 out–28 in	3 out–20 in	X	X	3 out–23 in	2 out–20 in	2 out–22 in	2 out–22 in	7 out–27 in	27 out–47 in	24 out–44 in	24 out–44 in	[23]
TSEG	8–32	7–32	5–29	2–23	2–22	2–23	3–25	2–21	3–25	2–25	4–28	24–49	21–46	21–46	[24]
hmmtop	7 out–28 in	6 out–25 in	6 out–27 in	3 out–21 in	2 in–20 out	2 in–20 out	5 out–23 in	2 in–20 out	2 in–23 out	2 in–23 out	2 in–26 out	23 out–47 in	20 out–44 in	20 out–44 in	[25]
MPEx	9–39	9–38	8–26	3–21	3–21	3–21	6–24	Short	5–48	5–23	12–30	29–47	26–44	26–44	[26]
Consensus (out–in)	8–29	7–28	7–28	3–21	3–21	3–21	4–23	2–21	3–24	3–23	7–27	25–46	23–43	22–44	

The amino acid loci of TMS taken for further studies is given in the bottom row, for the respective proteins (taken in columns)

This communication adopts a comprehensive approach to explore all the hypotheses above and attempts to find support in terms of biochemical logic or direct experimental evidence to ratify each hypothesis. We arrive at a conclusion that the N-termini could function as passive anchors for localizing and bringing CYP and CPR together in the phospholipid microenvironment.

Materials and Methods

Analysis of the N-termini for TMS

The N-terminal sequences of most of the published major and other minor mammalian (especially human) microsomal CYPs and CPR were collected from protein databases on the internet. Thirteen different programs (available online on servers from various research groups working on transmembrane peptide biochemistry [14–26], details of which are shown in Table 1) were used to predict the N-term TMS.

Probing Hetero-Recognitions Based on Available Phylogenetic and Structural Logic

TM*hit* server [27] was used for predicting N-terminal transmembrane helices "contact residue pairs" of CYP450 and CPR. This recently published methodology has been hitherto used for predicting contact residues of transmembrane helix (TMH) within a protein only. The consensus TMH sequences of CYP and CPR were taken in a single sequence pair so that its topology was in an "out–in–in–out" fashion within membrane. As a positive control, selected TMHs of aquaporin (1LDF), ATPase (1YCE) and bacteriorhodopsion (1C3W), which have known interactions, were also submitted to the same protocol. Some proteins containing helices which are known not to interact were sourced from the negatome database, and were used as negative controls (as exemplified by chains from cytochrome bc1 complex-1BE3). The results obtained from the server were then processed for better interpretation using an in-house written PERL script.

General Methodologies

Chemicals used in this study were purchased from reputed commercial suppliers and of analytical grade. Expression and purification of mammalian CYP and CPR was done as per published protocols [28, 29]. CYP (human CYP2C9 and rabbit 2E1) concentration was determined using the standard dithionite reduced carbon monoxide (CO) binding assay [30]. The intact CPR employed was a K56Q mutant to stabilize it from N-term proteolysis [31]. Flavin-based CPR quantification employed 10–20 μl of an appropriately diluted CPR stock in 10 μM ferricyanide at neutral pH. The concentration of CPR was determined by the optical density (OD) of the sample (OD 455–550 nm) divided by the molar extinction coefficient of 21,200 [32]. The four different CPR preparations (preps) were analyzed with sodium dodecyl sulfate polyacrylamide gel electrophoresis (SDS-PAGE) (10% polyacrylamide gel) to assess the extent of N-term scission. Densitometric analysis of the SDS-PAGE gel (Fig. A in the supplementary material) shows that the two (rabbit and human) CPR preps made from C41 and C-1a cells had only about 30 ± 2% (32 and 28%, respectively) intact CPR. In this study, they are also addressed as truncated (or broken) CPRa and CPRb, respectively. A prep of rabbit CPR from Top 3 cells had ~2/3 of the CPR intact and is referred to herein also as partly intact CPR. Another fresh prep of rabbit CPR from Top three cells showed no indication of scission of the N-term TMS, which is hereby referred to as intact CPR.

Reactions Employing Various CYP and CPR Preps

All reactions were carried out in open vials, with 100 mM potassium phosphate buffer, pH 7.4, incubated at 37°C. Unless otherwise mentioned, reconstituted systems had 10 μg/ml of 0.2 μm vesicles of dilauryl phosphatidylcholine (DLPC, Avanti Lipids). To 100 μl of the appropriate mixture of buffer stock and DLPC in distilled water, 20 μl each of the following four components was added: 1 μM human CYP2C9 (or 250 nM rabbit CYP2E1), 4 μM (or 1 μM) pertinent CPR, 2 μM (or 1 μM) cytochrome b_5 (if present, else 20 μl distilled water), 25 μM diclofenac [or 25 μM *para*-nitrophenol (pNP)] and the mixture was briefly equilibrated. Then, 20 μl of freshly prepared 5 mM NADPH was added and mixed to start the reaction. Therefore, CYP:cytochrome b_5 (when present):CPR was in the ratio of 1:2:4, respectively. Initial rates under steady-state conditions were monitored. Typically, 0.2–3 ml of the reaction mixture was taken initially and an appropriate volume taken out and quenched with a chilled reaction terminating solvent mixture. After centrifugation and filtration to remove any particulate matter, 20–50 μl of the sample was taken for product analysis by high performance liquid chromatography (HPLC). Details of HPLC methods to quantify 4′-hydroxydiclofenac (reaction product of CYP2C9 with diclofenac) and *para*-nitrocatechol (pNC, CYP2E1 reaction product of pNP) have been discussed in a recent communication from our lab [33]. Other specific details of concentrations and procedures are given in the respective legends.

Table 2 TMHs of some mammalian CYPs and CPRs

S. no.	NCBI Acc. no.	Protein	N-term sequence and TMH
1.	NP_000752.2	hCYP1A2	MALSQSV**PFSATELLLASAIFCLVFWVLK**GLRPRVPKLKSPPEPWGWPL
2.	NP_000758.1	hCYP2B6	ME**LSVLLFLALLTGLLLLLVQ**RHPNTHDRLPPGPRPLPLLGNLLQMDRRG
3.	NP_000762.2	hCYP2C9	MDS**LVVLVLCLSCLLLLSLWR**QSSGRGKLPPGPTPLPVIGNILQIGIKDI
4.	NP_000760.1	hCYP2C19	MD**PFVVLVLCLSCLLLLSIWR**QSSGRGKLPPGPTPLPVIGNILQIDIKDV
5.	ABB77909.1	hCYP2D6	MGL**EALVPLAMIVAIFLLLVDLM**HRRQRWAARYPPGPLPLPGLGNLLHVD
6.	AAF13598.1	hCYP3A4	MALIPD**LAMETWLLLAVSLVLLYLYGT**HSHGLFKKLGIPGPTPLPFLGNI
7.	NP_000764.1	hCYP2E1	M**SALGVTVALLVWAAFLLLVS**MWRQVHSSWNLPPGPFPLPIIGNLFQLEL
8.	NP_000932.3	hCPR	MINMGDSHVDTSSTVSEAVAEEVS**LFSMTDMILFSLIVGLLTYWF**LFRKK
9.	NP_001164592.1	rCYP1A2	MAMSPAA**PLSVTELLLVSAVFCLVFWAV**RASRPKVPKGLKRLPGPWGWPL
10.	P08682.2	rCYP2E1	MA**VLGITVALLGWMVILLFISVW**KQIHSSWNLPPGPFPLPIIGNLLQLDL
11.	NP_0001153762.1	rCPR	MADSHGDTGATMPEAAAQEAS**VFSMTDVVLFSLIVGLITYWFLF**RKKKEE
12.	NP_034123.1	mCYP1A2	MAFSQY**ISLAPELLLATAIFCLVFWMVR**ASRTQVPKGLKNPPGPWGLPFI
13.	NP_067257.1	mCYP2E1	MA**VLGITVALLVWIATLLLVSIWK**QIYRSWNLPPGPFPIPFFGNIFQLDL
14.	NP_032924.1	mCPR	MGDSHEDTSATVPEAVAEEVSL**FSTTDIVLFSLIVGVLTYWFI**FKKKKEE

The location of TMS (in bold) within the first 50 amino acids of the N-terminus is shown. The citations for the original sequence determination work could be accessed from the respective NCBI number

Results

Determination of N-term TMS, Topology Prediction, and Preliminary Analyses

To predict the putative TMS, the sequences of the first 50 amino acids of the N-term were fed to 13 servers on the internet. As shown in Table 1, at times, the exact location of the predicted TMH varied among the different methodologies. However, they were statistically in agreement with each other. The extracted segments were predicted to have a helical topology by MPEx [26], and neither β-sheet nor β-strand was seen. A consensus segment of $\sim$20 amino acids was thus derived for each CYP or CPR with N–C sequence in an out–in orientation. Table 2 (and Table A in the supplementary material) details the amino acid sequence and location of the predicted TMHs. CPR's TMH was highly conserved across the species studied. However, wide variations were observed within families and subfamilies of CYPs. For example, (a) the number of predictable TMS varied—none in 1A1 to three segments within the first 100 amino acids for 2E1, (b) the specific location of the first N-term TMS, inclusive of the signal peptide, and the length of hydropathy breaks varied and (c) the distribution of residues therein varied (JALView-Muscle or JALView-ClustalW alignment analyses did not show significant consensus within first 50 amino acids of the different CYPs).

TM*hit* Predictions for Interhelical Binding (Fig. 2)

The contact residue pairs for each N-terminal TM CYP–CPR helix pair were predicted from the TM*hit* server. In each CYP–CPR helix pair, a probability of 1 is taken for the residue pair with the highest confidence in the prediction. As these pairs are scored on the basis of relative confidence, probability scores of <0.9 may be considered unimportant. In an ideal case, the complete interacting faces of the helices that are in contact would have high probability values which would be visualized as a diagonal in the contact map. This is clearly visible for the positive controls, shown in three panels on the top row, left side. In the case of non-interacting helices, these interactions would be sparse, and not aligned along the face of the helix, as is seen in the data presented for the negative control in the single panel on top row, right. The remaining three rows of panels are for test interaction predictions for human CYP–CPR, mouse/rabbit CYP–CPR interactions, and cross-species CYP–CPR interactions, respectively. Out of several CYP–CPR combinations studied, most of the CYP–CPR contact pair residues' probabilities were usually <0.9, except a few exceptions. The test data show little tendency to form the diagonal pattern with high probability points (barring exceptions, like mCPR-mCYP1A2), indicating that there is little argument for a strong interaction. Apart from the CYP–CPR helical interaction predictions for major liver microsomal P450s, we had performed the same analyses for six other minor human P450s and two other rabbit and mouse P450s (Figs. B, C of the supplementary material). It is well-known that CPR works efficiently across species too. For example, rabbit CPR works quite well with human CYP2C9, a combination employed in this study. Prediction studies between human, rabbit, and mouse CPRs with alien CYPs 1A2 and 2E1 showed little scope for binding. (CYPs 1A2 and 2E1 were chosen as cross-species CYP representatives because these classes

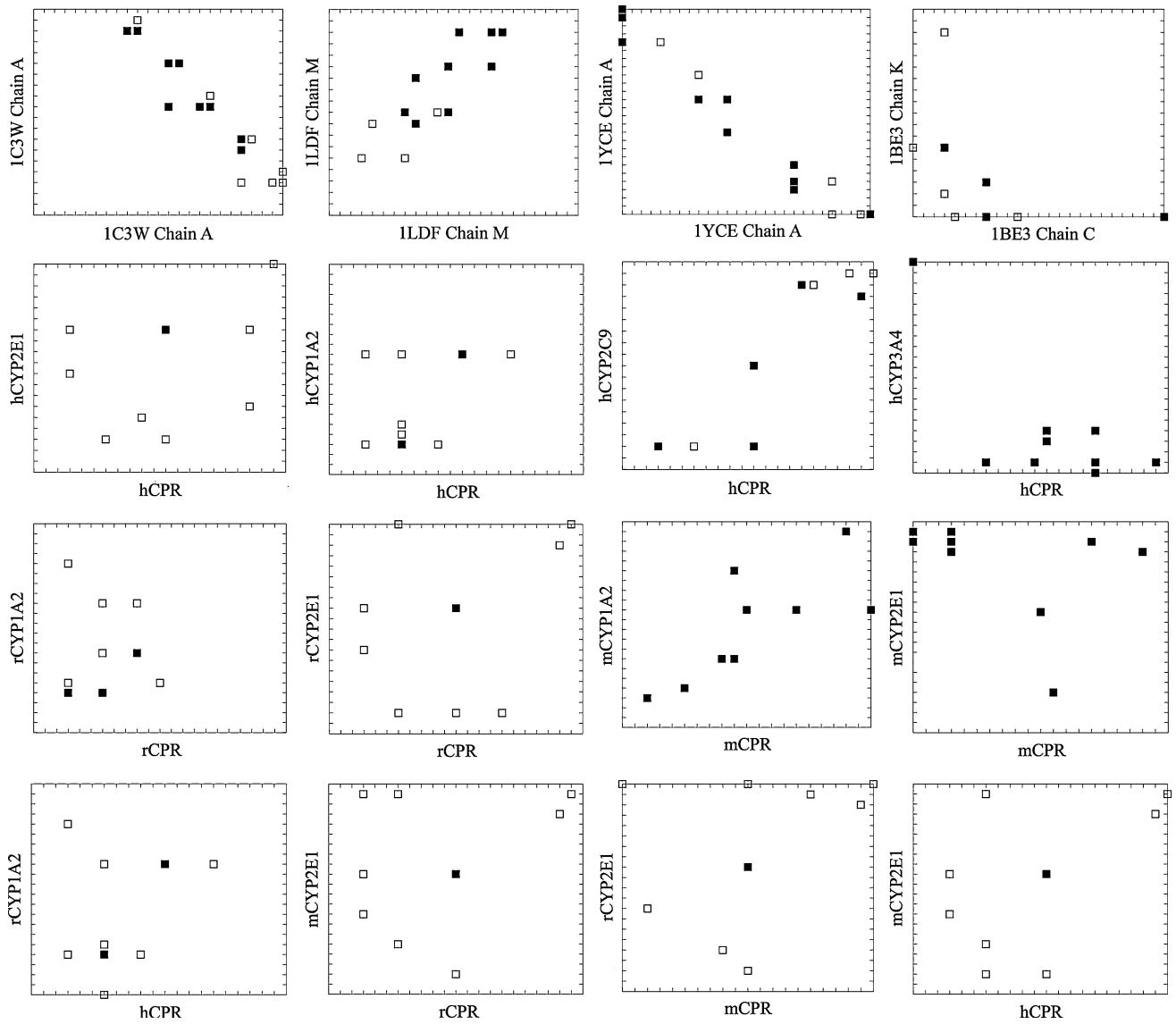

Fig. 2 TM*hit* results for TMH interactions between select mammalian liver microsomal CYPs and CPR. The *top row* shows the controls employed (three positives on the *left* and one negative on the *right*) and the remaining panels in the *bottom* three *rows* are test predictions between various mammalian CYPs and CPRs

of CYPs were present in fair consistency across the species.)

Mammalian CPR Preps Employed for In Vitro Studies in the Current Work

Equal amounts of four different CPR preps (as estimated by flavin spectrum) with varying extents of N-term integrity were used for carrying out reactions.

Effect of Cytochrome b_5 on Various CPR preps' Activities with Human CYP2C9

All four CPR preps were separately employed for carrying out the hydroxylation of diclofenac in reconstituted CYP2C9 systems and the results are shown in Fig. 3. The intact N-term CPR showed highest activities in the control as well as the reaction employing cytochrome b_5. However, the point to be clearly noted was that the extent of integrity was not directly correlated to the specific reaction product in control or test reactions. In controls, the truncated CPR preps (CPRa, CPRb) and partly intact CPR, respectively, gave $\sim$13% (lower than expected), 47% (higher than expected), and 36% (lower than expected) of the intact CPR's activity. Incorporation of cytochrome b_5 gave surprising results—the activity of the two truncated CPR preps (CPRa and CPRb) and partly intact CPR was $\sim$36% (roughly equal to expected, increased relative to control lacking cytochrome b_5 for the same reaction), 19% (lower than expected, decreased relative to control lacking

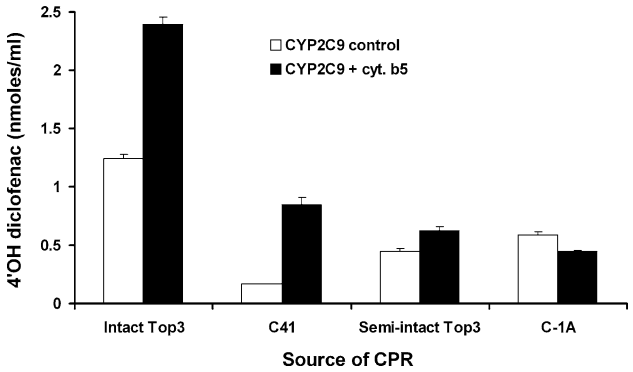

Fig. 3 The effect of employing various CPR preps and cytochrome b_5 on CYP2C9-mediated hydroxylation of diclofenac. The initial concentration of reaction components were: [CYP2C9] = 100 nM, [CPR] = 400 nM, [cytochrome b_5, when present] = 200 nM, [diclofenac] = 25 μM, [NADPH] = 500 μM. The amount of specifically hydroxylated product 4′-hydroxydiclofenac formed after 8 min of reaction is plotted

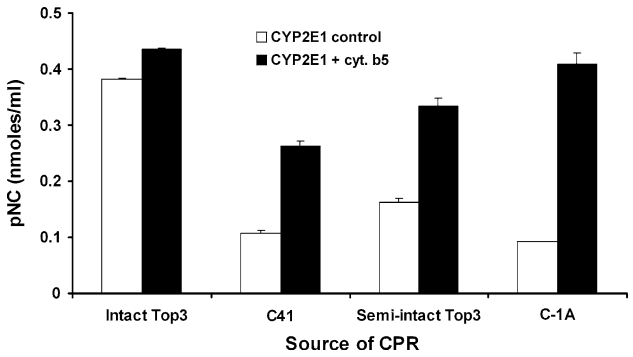

Fig. 4 The effect of employing various CPR preps and cytochrome b_5 on CYP2E1-mediated hydroxylation of *p*-nitrophenol. The initial concentration of reaction components were: [CYP2E1] = 25 nM, [CPR] = 100 nM, [cytochrome b_5, when present] = 50 nM, [pNP] = 25 μM, [NADPH] = 500 μM. The amount of specifically hydroxylated product pNC formed after 8 min of reaction is plotted

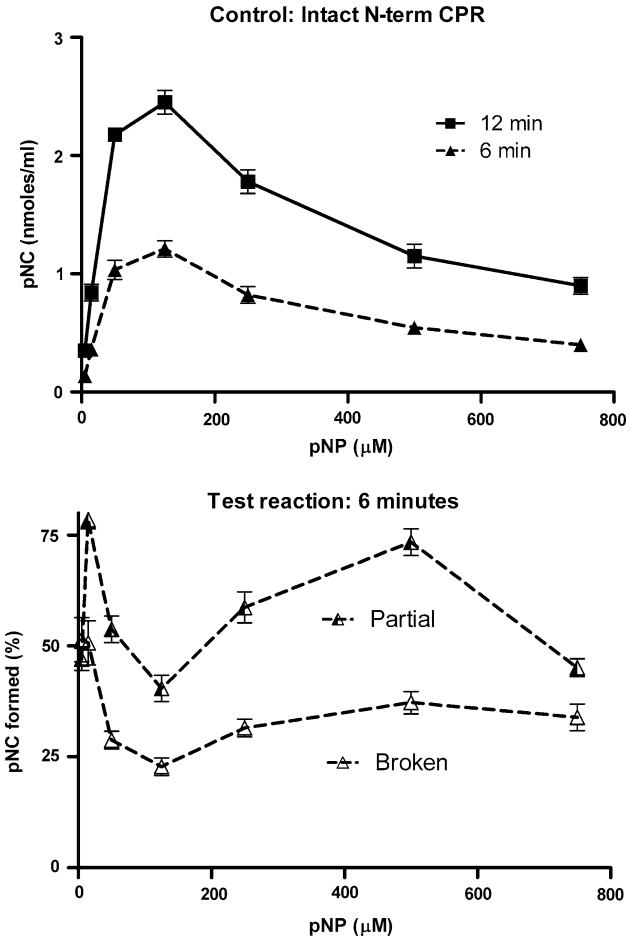

Fig. 5 The effect of employing various CPR preps and varying pNP (substrate) concentration on CYP2E1-mediated hydroxlations. The initial concentration of reaction components were: [CYP2E1] = 15 nM, [CPR] = 60 nM, [cytochrome b_5] = 50 nM, [NADPH] = 500 μM. The data for the controls is shown for extended period so that it is clearly understood that the reaction regime is within steady-state conditions

cytochrome b_5 for the same reaction), and 26% (lower than expected, increased relative to control lacking cytochrome b_5 for the same reaction) of the intact CPR's activity.

Effect of Cytochrome b_5 on Various CPR preps' Activities with Rabbit CYP2E1

The four CPR preps were separately employed for carrying out the hydroxylation of pNP in reconstituted CYP2E1 systems. The results are shown in Fig. 4. Again, the intact CPR showed highest activities in the control as well as the reaction employing cytochrome b_5. It was clearly noted yet again that the extent of integrity was not directly correlated to the specific reaction product in control or test reactions. In controls, the truncated CPR preps (CPRa, CPRb) and partly intact CPR, respectively, gave 28% (roughly expected), 24% (roughly expected), and 43% (lower than expected) of intact CPR's activity. Incorporation of cytochrome b_5 yet again gave surprising results—the activity of the two truncated CPR preps and partly intact CPR were 60% (higher than expected, increased relative to the control lacking cytochrome b_5 for the same reaction), 94% (higher than expected, increased relative to control lacking cytochrome b_5 for the same reaction), and 77% (roughly expected, increased relative to control lacking cytochrome b_5 for the same reaction) of the control reaction.

CPR preps' Activities Obtained with CYP2E1 by Varying Substrate Concentration

Here, the activity of the soluble CPRa, (1/3 intact), CPRb (<1/3 intact) and partly intact CPR preps is compared with

the activity of fully intact CPR. The results are shown in Fig. 5. At a substrate concentration of 5 μM, both the soluble and partly intact CPR preps gave roughly equal (~51 and 47%, respectively) activity, with respect to the control reaction incorporating the fully intact CPR. From the expected values, these values are much higher for the soluble prep and lower for the partly intact prep. At 15 μM pNP, the same preps gave 51 and 78% activity, respectively, with respect to the intact CPR reaction. These values are higher than the expected value for both preps. At 750 μM pNP, the preps showed 34% (roughly expected value) and 45% (lower than expected value) activity, respectively. At the other substrate concentration ranges, as expected, the partly intact CPR prep showed double the activity of soluble CPRa prep. However, the absolute percentages of values with respect to the control varied significantly. For example, the partly intact CPR prep gave activities ranging from 40 to 74% within the 15–750 μM substrate concentration regimes.

Discussion

Depending on the depth of the lamellum (formed with fatty acyl chain lengths of 12–22 carbons, translating to ~17–34 Å) and the inherent composition of the peptide backbone, a TM traversing helix's length could vary. Usually, it ranges from 15 to nearly around 20 amino acid residues, with a typical length of 19–20 as an upright TM helix [34, 35]. Tryptophan and proline could serve as a surface anchor [36]. "Positive inside rule" says that segment of TMS having amino acids with positively charged R groups are present in the cytoplasmic side [37]. Topology prediction and modeling macromolecular interactions within the transmembrane domain remains a highly emerging and speculative field, constantly inundated with new ideas. Computational measurements for normal docking procedures involve maximizing the van der Waals and electrostatic contributions to the energy function. These are inadequate for an accurate prediction of protein–protein interactions, since the proteins may be fairly flexible. Currently, little factual knowledge about inter-protein TMH interactions is available. Since TMS are predominantly hydrophobic structures embedded in a hydrophobic phospholipid microenvironment [38], one could envisage the formation of a predictably stable complex by the chemical logic of disulfide bonds, salt bridges, hydrogen bonds, and pi–pi stacking [37]. Researchers in the area have also endorsed special cases like—serine zippers, (i, $i + 4$) sequences, Ile/Val/Leu patches, or small residue close packing [39, 40]. A simple qualitative survey of the TMS (as shown in Table 2) do not present strong arguments along the above lines for supporting the binding of CYPs and CPR within the same species or across species. Only, instances with scope for putative pi-stacking or hydrogen bonding could be found, a maximal of one each in a given CYP–CPR pairing.

Since crystal structures of some membrane multimeric proteins are available, we used the inter-chain binding within these proteins as a reference for inter-protein TMH-bindings. This is because the logic of binding would be similar in both the cases. For the purpose of predicting interacting residues between TMHs, we have used the TM*hit* server [27], which is a Kernel method (Support Vector Machine). It is built by using known interacting residues and non-interacting residues as a training data set and can assign a probability value to a contact pair. For further analysis, we plotted the results as a contact plot, from which interacting faces in the two helices could be clearly interpreted. The liver microsomal CYP–CPR binding predictions showed fewer contact points with lower probability values and a dispersion of the same (as opposed to the diagonal pattern for positive control), for an overwhelming majority of combinations studied. We also found that the results obtained for TM*hit* predictions for other minor liver microsomal P450s and CPR (six human CYPs-human CPR, two rabbit CYPs-rabbit CPR, and two mouse CYPs-mouse CPR combinations, Figs. B, C of the supplementary material) were similar to the predictions obtained for major P450s studied herein. This finding re-enforces the analyses drawn from the preliminary analyses of TMS of CYP and CPR that there is little evidence or reason to suppose that a conserved CPR's TMS could rest the merit to interact selectively with the various CYPs' TMS, within and across species. It had been noted that N-term truncated P450 expressed in bacteria and other systems could express functional P450 protein. Also, several reports affirm that the expression and activity of truncated P450s does not significantly alter their kinetic profiles or perturb their spectral properties [41–47]. In fact, the CYP2C9 employed in this study was expressed as a poly his-tag protein in *E. coli* for convenience in purification. A study has also revealed that human liver microsomal cytosolic fractions contained a catalytically active N-term truncated soluble CYP3A4 [48]. Therefore, the hypothesis that CYP's N-term TMS could be involved in hetero-recognition with CPR's N-term TMH (Hypothesis 1) is conclusively rendered invalid.

Next, we look into Hypothesis 2, which vouches for the involvement of CPR's N-term in active site. Venkateswarlu et al. [46] had recently found that CPR's N-term is not required for the CPR activity or reconstitution of CYP activity in situ, within a yeast system. However, this finding could be downplayed by arguments of heterologous expression incompatibilities [43]. Clearly, our in vitro experiments with the four CPR preps (Figs. 3, 4) show that

the preps lacking the intact N-term could also afford significant functionality. What could be factually inferred from our experiments is that: (1) under certain experimental conditions, the presence of free N-term TMS in the reaction medium could be detrimental to activity and (2) mostly, intact CPR gave generally better activities (were better coupled) than truncated CPR. Therefore, an obligatory role for CPR's N-term TMS can be downplayed. Therefore, Hypothesis 2 is effectively annulled.

Recently published work [49] on Nox, a membrane flavoprotein akin to CPR, is very relevant to the understanding of phenomenon seen in Figs. 3, 4, and 5. Working on Nox-4, Ralf Brandes' group found that deletion of the E-loop or mutation of a conserved histidine within that stretch switched Nox-4 from an H_2O_2 generating system to an $O_2^{\cdot-}$ generating system. Their work clearly implies that the E-loop, a peripheral component of the flavoprotein, is involved in diffusible reduced oxygen species (DROS, as exemplified by H_2O_2 and $O_2^{\cdot-}$) dynamics. Also, some reports of perturbation of Nox activity by synthetic peptides bearing positively charged amino acid residues [50, 51] could be considered analogous to the observations of Minor Coon's group, who noted that N-term portions of trypsinized CPR leading to a decrease in the substrate hydroxylation [4, 5]. This is because the N-term proteolytically cleavable TMS of CPR possesses positively charged residues (His and Lys). We have recently invoked on DROS dynamics to explain for several novel and hitherto poorly understood phenomena in heme-enzyme reaction environments [32, 33]. We have shown that the incorporation of cytochrome b_5 and altering the concentration of the final substrate modulates the DROS dynamics in heme-enzyme reactions [32, 33]. Putting the findings on Nox and our works together, we could interpret our findings (Figs. 3, 4, 5) as an outcome of the DROS dynamics. CPR's N-term could affect product formation because when free, it could alter the DROS dynamics in the reaction microenvironment. Incorporation of cytochrome b_5 or altering substrate concentration could potentially offset this effect, under certain reaction regimes [33]. Presence of redox-active additives in the enzyme preps could also lead to chaotic perturbances of the reaction outcome [52, 53], which could explain the difference in activity between the various preps.

To conclude, our findings and arguments support the Hypothesis 3, as shown in Fig. 1. The phospholipid bilayer, a relatively two-dimensional and constrained space, enhances the probability of catalysis/interactions by localizing and bringing the CYP and CPR in proximity to each other. We also provide indirect evidence for the impact and involvement of DROS in the reaction microenvironment. We are currently investigating the competing reactions within the microenvironment and chartering the roles of DROS in CYP–CPR-mediated catalysis.

Acknowledgments KMM thanks Dr. Manish Bharadwaj, Wake Forest University, North Carolina (for assisting in densitometry) and the Department of Chemistry, Washington State University. This research was funded by VIT University, NIH grants GM32165 and "Satyamjayatu: The Science Foundation."

References

1. Ortiz de Montellano, P. R. (Ed.). (2005). *Cytochrome P450: Structure, mechanism and biochemistry* (3rd ed.). New York: Plenum Press.
2. Coon, M. J. (2005). Cytochrome P450: Nature's most versatile biological catalyst. *Annual Reviews in Pharmacology and Toxicology, 45*, 1–25.
3. Estabrook, R. W., Franklin, M. R., Cohen, B., Shigmatzu, A., & Hildebrandt, A. G. (1971). Influence of hepatic microsomal mixed function oxidation reactions on cellular metabolic control. *Metabolism, 20*, 187–199.
4. Black, S. D., French, J. S., Williams, C. H., & Coon, M. J. (1979). Role of a hydrophobic polypeptide in the N-terminal region of NADPH-cytochrome P450 reductase in complex formation with $P450_{LM}$. *Biochemical and Biophysics Research Communications, 91*, 1528–1535.
5. French, J. S., Black, S. D., Williams, C. H, Jr, & Coon, M. J. (1980). Studies on the association of $P450LM_2$ with NADPH cytochrome P450 reductase and with tryptic peptides derived from the reductase. In M. J. Coon, A. H. Conney, R. W. Estabrook, H. V. Gelboin, J. R. Gillette, & P. J. O'Brien (Eds.), *Microsomes, drug oxidations and chemical carcinogenesis*. New York: Academic Press.
6. Gum, J. R., & Strobel, H. W. (1981). Isolation of the membrane binding peptide of NADPH cytochrome P450 reductase. *The Journal of Biological Chemistry, 256*, 7478–7486.
7. Black, S. D., & Coon, M. J. (1981). Structural features of liver microsomal NADPH-cytochrome P-450 reductase. *The Journal of Biological Chemistry, 257*, 5929–5938.
8. Lewis, D. F. V. (1995). Three-dimensional models of human and other mammalian microsomal P450s constructed from an alignment with P450102 (P450bm3). *Xenobiotica, 25*, 333–366.
9. Müller-Enoch, D., & Gruler, H. (2000). Complexation of membrane-bound enzyme systems. *Zeitschrift für Naturforschung C: Journal of Biosciences, 55*, 747–752.
10. Yang, C. S. (1977). Interactions between solubilized cytochrome P450 and hepatic microsomes. *The Journal of Biological Chemistry, 252*, 293–298.
11. Kaminsky, L. S., & Guengerich, F. P. (1985). Cytochrome P-450 isozyme/isozyme functional interactions and NADPH-cytochrome P-450 reductase concentrations as factors in microsomal metabolism of warfarin. *European Journal of Biochemistry, 149*, 479–489.
12. Finch, S. A. E., & Stier, A. (1991). Rotational diffusion of homo- and hetero-oligomers of cytochrome P-450, the functional significance of cooperativity and the membrane structure. *Frontiers in Biotransformation, 5*, 34–70.
13. Brignac-Huber, L. M., Reed, J. R., & Backes, W. L. (2011). Organization of NADPH-cytochrome P450 reductase and CYP1A2 in the endoplasmic reticulum-microdomain localization affects monooxygenase function. *Molecular Pharmacology, 79*, 3549–3557.
14. Pashou, E. E., Litou, Z. I., Liakopoulos, T. D., & Hamodrakas, S. J. (2004). waveTM: Wavelet-based transmembrane segment prediction. *In Silico Biology, 4*, 127–131.

15. Hofmann, K., & Stoffel, W. (1993). TMbase—A database of membrane spanning proteins segments. *Biological Chemistry Hoppe-Seyler, 374*, 166.
16. von Heijne, G. (1992). Membrane protein structure prediction, hydrophobicity analysis and the positive-inside rule. *Journal of Molecular Biology, 225*, 487–494.
17. Cserzo, M., Wallin, E., Simon, I., von Heijne, G., & Elofsson, A. (1997). Prediction of transmembrane alpha-helices in prokaryotic membrane proteins: The dense alignment surface method. *Protein Engineering, 10*, 673–676.
18. Hirokawa, T., Boon-Chieng, S., & Mitaku, S. (1998). SOSUI: Classification and secondary structure prediction system for membrane proteins. *Bioinformatics, 14*, 378–379.
19. Krough, A., Larsson, B., von Heijne, G., & Sonhammer, E. L. (2001). Predicting transmembrane protein topology with a hidden Markov model: Application to complete genomes. *Journal of Molecular Biology, 305*, 567–580.
20. Pasquier, C., Promponas, V. J., Palaios, G. A., Hamodrakas, J. S., & Hamodrakas, S. J. (1999). A novel method for predicting transmembrane segments in proteins based on a statistical analysis of the Swiss Prot database: The PRED-TMR algorithm. *Protein Engineering, 12*, 381–385.
21. Schultz, J., Milpetz, F., Bork, F., & Ponting, C. P. (1998). SMART, a simple modular architecture research tool: Identification of signaling domains. *Proceedings of the National Academy of Sciences of the United States of America, 95*, 5857–5864.
22. Juretic, D., Zoranic, L., & Zucic, D. (2002). Basic charge clusters and predictions of membrane protein topology. *Journal of Chemical Informatics and Computer Science, 42*, 620–632.
23. Kahsay, R., Liao, L., & Gao, G. (2005). An improved Hidden Markov Model for transmembrane protein detection and topology prediction and its applications to complete genomes. *Bioinformatics, 21*, 1853–1858.
24. Kihara, D., Shimizu, T., & Kanehisa, M. (1998). Prediction of membrane proteins based on classification of transmembrane segments. *Protein Engineering, 11*, 961–970.
25. Tusnády, G. E., & Simon, I. (1998). Principles governing amino acid composition of integral membrane proteins: Applications to topology prediction. *Journal of Molecular Biology, 283*, 489–506.
26. Snider, C., Jayasinghe, S., Hristova, K., & White, S. H. (2009). MPEx: A tool for exploring membrane proteins. *Protein Science, 18*, 2624–2628.
27. Lo, A., Chiu, Y. Y., Rødland, E. A., Lyu, P. C., Sung, T. Y., & Hsu, W. L. (2009). Predicting helix–helix interactions from residue contacts in membrane proteins. *Bioinformatics, 25*, 996–1003.
28. Collom, S. L., Jamakhandi, A. P., Tackett, A. J., Radominska-Pandya, A., & Miller, G. P. (2007). CYP2E1 active site residues in substrate recognition sequence 5 identified by photoaffinity labeling and homology modeling. *Archives of Biochemistry and Biophysics, 459*, 59–69.
29. Cheng, D., Kelley, R. W., Cawley, G. F., & Backes, W. L. (2004). High-level expression of recombinant rabbit cytochrome P450 2E1 in *Escherichia coli* C41 and its purification. *Protein Expression and Purification, 33*, 66–71.
30. Omura, T., & Sato, R. (1964). The carbon monoxide-binding pigment of liver microsomes: Evidence for its hemoprotein nature. *The Journal of Biological Chemistry, 239*, 2370–2378.
31. Bonina, T. A., Gilep, A. A., Estabrook, R. W., & Usanov, S. A. (2005). Engineering of proteolytically stable NADPH-cytochrome P450 reductase. *Biochemistry, 70*, 357–365.
32. Manoj, K. M., Gade, S. K., & Mathew, L. (2010). Cytochrome P450 reductase: A harbinger of diffusible reduced oxygen species. *PLoS One, 5*(10), e13272. doi:10.1371/journal.pone.0013272.
33. Manoj, K. M., Baburaj, A., Ephraim, B., Pappachan, F., Maviliparambathu, P. P., Vijayan, U. K., et al. (2010). Explaining the atypical reaction profiles of heme enzymes with a novel mechanistic hypothesis and kinetic treatment. *PLoS One, 5*(5), e10601. doi:10.1371/journal.pone.0010601.
34. Lewis, D. F. V. (Ed.). (1996). *Cytochromes P450: Structure, function and mechanism*. London: Taylor & Francis.
35. Von Heijne, G., & Gavel, Y. (1988). Topogenic signals in integral membrane proteins. *European Journal of Biochemistry, 174*, 671–678.
36. Abell, B. M., & Mullen, R. T. (2011). Tail-anchored membrane proteins: Exploring the complex diversity of tail-anchored-protein targeting in plant cells. *Plant Cell Reports, 30*, 137–151.
37. Chen, C. P., & Rost, B. (2002). State-of-the-art in membrane protein prediction. *Applied Bioinformatics, 1*, 21–35.
38. Helms, V. (2002). Attraction within the membrane: Forces behind transmembrane protein folding and supramolecular complex assembly. *EMBO Reports, 3*, 1133–1138.
39. Harrington, S. E., & Ben-Tal, N. (2009). Structural determinants of transmembrane helical proteins. *Structure, 17*, 1092–1103.
40. Popot, J. L., & Engelman, D. M. (2000). Helical membrane protein folding, stability and evolution. *Annual Reviews of Biochemistry, 69*, 881–922.
41. Li, Y. C., & Chiang, J. Y. L. (1991). The expression of a catalytically active cholesterol 7alpha-hydroxylase cytochrome P450 in *Escherichia coli*. *The Journal of Biological Chemistry, 266*, 19186–19191.
42. Larson, J. R., Coon, M. J., & Porter, T. D. (1991). Purification and properties of a shortened form of Cytochrome P-450 2E1: Deletion of the NH_2-terminal membrane-insertion signal peptide does not alter the catalytic activities. *Proceedings of the National Academy of Sciences of the United States of America, 88*, 9141–9145.
43. Sagara, Y., Barnes, H. J., & Waterman, M. R. (1993). Expression in *Escherichia coli* of functional cytochrome P450cl7 lacking its hydrophobic amino-terminal signal anchor. *Archives of Biochemistry and Biophysics, 304*, 272–278.
44. Kempf, A. C., Zanger, U. M., & Meyer, U. A. (1995). Truncated human P450 2D6: expression in *Escherichia coli*, Ni (2+)-chelate affinity purification, and characterization of solubility and aggregation. *Archives of Biochemistry and Biophysics, 321*, 277–288.
45. Von Wachenfeldt, C., Richardson, T. H., Cosme, J., & Johnson, E. F. (1997). Microsomal P450 2C3 is expressed as a soluble dimer in *Escherichia coli* following modifications of its N-terminus. *Archives of Biochemistry and Biophysics, 339*, 107–114.
46. Venkateswarlu, K., Lamb, D. C., Kelly, D. E., Manning, N. J., & Kelly, S. L. (1998). The N-terminal membrane domain of yeast NADPH-cytochrome P450 (CYP) oxidoreductase is not required for catalytic activity in sterol biosynthesis or in reconstitution of CYP activity. *The Journal of Biological Chemistry, 273*, 4492–4496.
47. Cosme, J., & Johnson, E. E. (2000). Engineering microsomal cytochrome P450 2C5 to be a soluble, monomeric enzyme: Mutations that alter aggregation, phospholipid dependence of catalysis, and membrane binding. *The Journal of Biological Chemistry, 28*, 2545–2553.
48. Jeon, S., Kim, K. H., Yun, C. H., Hong, B. W., Chang, Y. S., Han, H. S., et al. (2008). An NH_2-terminal truncated cytochrome P450 CYP3A4 showing catalytic activity is present in the cytoplasm of human liver cells. *Experimental and Molecular Medicine, 40*, 254–260.
49. Takac, I., Schröder, K., Zhang, L., Lardy, B., Anilkumar, N., Lambeth, J. D., et al. (2011). The E-loop is involved in hydrogen peroxide formation by the NADPH oxidase Nox4. *The Journal of Biological Chemistry, 286*, 13304–13313.

50. Joseph, G., Gorzalczany, Y., Koshkin, V., & Pick, E. (1994). Inhibition of NADPH oxidase activation by synthetic peptides. *The Journal of Biological Chemistry, 269*, 29024–29031.
51. El-Banna, J., Dang, P. M. C., & Perianin, A. (2010). Peptide based inhibitors of the phagocyte NADPH oxidase. *Biochemical Pharmacology, 80*, 778–785.
52. Andrew, D., Hager, L. P., & Manoj, K. M. (2011). The intriguing enhancement of chloroperoxidase mediated one-electron oxidations by azide, a known active-site ligand. *Biochemical Biophysical Research Communications, 415*, 646–649.
53. Parashar, A., & Manoj, K. M. (2011). Traces of certain drug molecules could enhance heme-enzyme catalytic outcomes. *Biochemical Biophysical Research Communications, 417*, 1041–1045.